Organic Molecules in Interstellar Space: Latest Advances

Michel Guélin[1]* and Jose Cernicharo[2]

[1]Institut de RadioAstronomie Millimétrique, St Martin d'Hères, France, [2]Instituto de Física Fundamental, Madrid, Spain

Although first considered as too diluted for the formation of molecules *in-situ* and too harsh an environment for their survival, the interstellar medium has turned out to host a rich palette of molecular species: to date, 256 species, not counting isotopologues, have been identified. The last decade, and more particularly the last 2 years, have seen an explosion of new detections, including those of a number of complex organic species, which may be dubbed as prebiotic. Organic molecules have been discovered not just in interstellar clouds from the Solar neighbourhood, but also throughout the Milky-Way, as well as in nearby galaxies, or some of the most distant quasars. These discoveries were made possible by the completion of large sub-millimetre and radio facilities. Equipped with new generation receivers, those instruments have provided the orders of magnitude leap in sensitivity required to detect the vanishingly weak rotational lines that allowed the molecule identifications. Last 2 years, 30 prebiotic molecules have been detected in TMC-1, a dust-enshrouded gaseous cloud located at 400 light-years from the Sun in the Taurus constellation. Ten new molecular species, have been identified in the arm of a spiral galaxy seven billion light-yr distant, and 12 molecular species observed in a quasar at 11 billion light-yr. We present the latest spectral observations of this outlying quasar and discuss the implications of those detections in these 3 archetypal sources. The basic ingredients involved in the Miller-Urey experiment and related experiments (H_2, H_2O, CH_4, NH_3, CO, H_2S, ...) appeared early after the formation of the first galaxies and are widespread throughout the Universe. The chemical composition of the gas in distant galaxies seems not much different from that in the nearby interstellar clouds. It presumably comprises, like for TMC-1, aromatic rings and complex organic molecules putative precursors of the RNA nucleobases, except the lines of such complex species are too weak to be detected that far.

Keywords: interstellar matter (ISM), molecules—ISM, galaxies, astrochemistry, radio astronomy, prebiotic molecules

1 INTRODUCTION

The question of extraterrestrial life arose as soon as Earth was recognized as one amid a myriad of celestial bodies. At first, alien life was fancied as a mere mirror of the life on Earth, with living creatures possibly scaled to the size of their home planets [see *L'autre Monde* by Savinien de Cyrano de Bergerac, printed in 1657, *Cosmotheoros* by Huygens (1698), and *Micromégas* by Voltaire (1752)]. Later, advances in science let writers realize that aliens may not look so friendly (*The War of the Worlds*, H.G. Wells). Finally, it was argued that extraterrestrial life could be based on silicium or germanium, instead of carbon, and take surprising forms. The most imaginative along this line was F.

Hoyle who published, sharp 300 years after Cyrano's book, a novel that invokes an interstellar cloud as a living being: *The Black Cloud* (Hoyle, 1957). Sir Fred Hoyle, whose grand reputation stems from his elucidation of the origin of carbon and heavier elements (Burbidge et al., 1957), but also from his taste for unorthodox theories, was a defender of panspermia and a forceful opponent of Earth-based abiogenesis.

The panspermia hypothesis, first developed in the 19th century, assumes that life came from outer space in the form of microscopic organisms present on meteorites or dust particles that somehow survived their impact on the Earth. In Hoyle's view, the great advantage of panspermia was that it immensly increases the time, hence the probability, for a chance assembly of atoms into prebiotic molecules within the lifetime of a (in his view) Steady State Universe.

Subsequent discoveries have shown that such a process has occured for at least some prebiotic building blocks. The first interstellar molecules (CH, CN, CH$^+$) were discovered in the optical spectra of nearby stars (Swings and Rosenfeld 1937; McKellar 1940; Douglas and Herzberg 1941), but it took 30 years until more complex species (e.g., NH$_3$ Cheung et al., 1968) could be found in interstellar space. In echo to Hoyle's science-fiction novel, water and formaldehyde, the first organic molecule, were detected in 1969 and found ubiquitous in interstellar clouds (Cheung et al., 1969; Snyder et al., 1969). The construction of the large (36-ft diameter) radio-telescope on Kitt Peak, Arizona, and of the Bell Laboratories first Schottky barrier diode receiver fitted for millimetre-wave observations, opened the way to a surge of new discoveries: CO, the most abundant interstellar molecule after H$_2$ (Wilson et al., 1970), hydrogen sulfide H$_2$S, the first alcohol CH$_3$OH, ethanol, ... This firework led Patrick Thaddeus, key actor on this scene, to state the Fisher's Scientific Principle: *If you can't find it at the Fisher Chemical store you will not find it in the interstellar gas* (Thaddeus, 2006). This statement, however, was soon overturned by William Klemperer and Thaddeus' own NASA team by the discovery of the first *non-terrestrial* molecular species: protonated carbon monoxyde HCO$^+$, protonated nitrogen N$_2$H$^+$, CCH, C$_3$N, and C$_4$H (Green et al., 1974; Herbst and Klemperer, 1974; Tucker et al., 1974; Guélin and Thaddeus, 1977; Guélin et al., 1978), all five unstable species not previoulsy observed in the laboratory.

To date, 256 molecular species, not counting isotopologues, are identified in interstellar clouds and circumstellar shells (see references hereafter). They are mostly acyclic organic molecules or radicals with C-chain backbones, as well as half a dozen rings with 5–10 C-atoms. They include aldehydes, alcohols, acids, amines and carboxamides, i.e. the main functional groups needed to initiate the formation of prebiotic molecules and RNA.

It is worth noting that no amino acid has been found to date in interstellar space, despite multiple searches for glycine (NH$_2$-CH$_2$-COOH), the simplest of them (Guélin and Cernicharo, 1989; Snyder et al., 2005; Jimenez-Serra et al., 2020). On the other hand, four putative precursors of glycine, methylamine (CH$_3$NH$_2$–Holtom et al., 2005), formamide (CH$_3$CHO – Rubin et al., 1971; Ferus et al., 2018), glycolonitrile (HOCH$_2$CN –Zeng et al., 2019) and aminoacetonitrile (NH$_2$-CH$_2$-CN—Belloche et al.,

2008), are detected, as is cyanomethanimine (HNCHCN—Rivilla et al., 2019) a HCN dimer and possible precursor of adenine, H$_5$C$_5$N$_5$, one of the four nucleobases of DNA.

The increasing rate of new detections mainly stems from advances in spectroscopic and astronomical instrumentation. Progress has been particularly striking in the sub-millimetre and radio domains. Those wavelenghts cover the lowest rotational lines of molecules of astrochemical interest and allow radiation to freely transit through dust-enshrouded clouds. In **Section 2**, we describe the state-of-the-art instrumentation used in current molecule searches. In **Section 3** and **Section 4**, we present recent results based on extensive spectral surveys of 3 archetypal interstellar sources: first a cold dark cloud, not unlike Hoyle's *Black Cloud*, in the Solar vicinity, then the spiral arm of a galaxy located 7 billion light-years away, finally a remote quasar at a time when the Universe was only 2.7 billion light-years old.

2 DETECTORS AND TELESCOPES AT MM/SUB-MM WAVELENGTHS

In the last decade, the field of astrochemistry has seen major advances triggered by the completion of new powerful radio telescopes, such as the Atacama Large sub-Millimetre Array (ALMA) and the Northern Extended Millimetre Array (NOEMA), coupled to impressive gains in sensitivity of receivers and in bandwidth. We here briefly review the leading facilities and their new equipment that allowed the latest progress in searching for new molecules in interstellar space.

The gains in detector sensitivity and bandwidth were linked to the development of low-noise/wide-band cryogenic amplifiers, based on HEMTs (High Electron Mobility Transistors) that operate around 15 K, and the development of mixers equipped with SIS (Superconductor-Insulator-Superconductor) junctions, based on photon-assisted electron tunneling at temperatures below 4 K. State of the art heterodyne receivers equipped with such devices now achieve noise temperatures of only few times the quantum limit ($2h\nu/k$), hence close to optimal, and ally increasingly wide tuning ranges and instantaneous bandwidths.

The heterodyne technique is based on the down-conversion of the incoming Radio Frequency (RF) signal (astronomical or from laboratory) resulting from its mixing with the narrow signal of a local oscillator. The lower frequency allows to use lower noise amplifiers and, mostly, provides a spectral resolution equal to the local oscillator line width, in practice better than 10^{-8} of the RF frequency. Whereas high sensitivity is needed for detecting the vanishingly weak rotational line emission from rare molecular species, or from very distant sources, high spectral resolution is crucial to identify with certainty the carriers of detected astronomical lines. Similarly, high spectral resolution is needed in the spectroscopic laboratory to accurately measure the rotational line pattern, hence derive the spectroscopic constants.

On the backend side, the availability of increasingly high-speed ADCs (Analog-to-Digital Converters) and powerful FPGAs (Field-programmable Gate Arrays) have allowed the

FIGURE 1 | The IRAM 30-m diameter millimeter-wave telescope operating on Pico Veleta in the Sierra Nevada, Spain, at 2,900 m altitude.
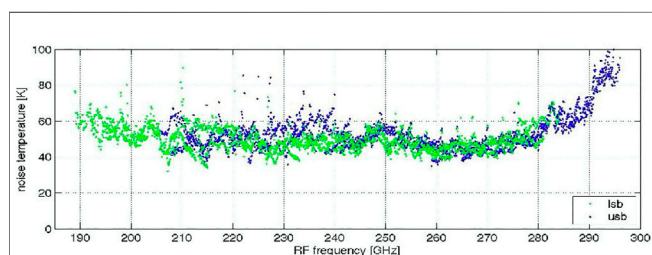

FIGURE 2 | Noise temperature in the lower (green dots) and upper (blue dots) sidebands of the 2SB SIS mixer receiver on the 30-m telescope—credit: D. Maier, IRAM.

development of digital correlators that process increasingly wide bandwidths, while keeping high spectral resolution.

The EMIR SIS junction receivers on the IRAM 30-m diameter telescope, located at an altitude of 2,900 m on Pico Veleta, near Granada, Spain (**Figure 1**), allow to simultaneously observe a 32 GHz-wide band with a spectral resolution of 200 kHz within the 73–375 GHz (λ 4 to 0.8 mm) atmospheric windows. Their intrinsic noise within this band varies between 2.5 and 5 times the quantum noise limit (**Figure 2**). The K-band HEMT receivers on the 100-m Green Bank telescope, which can observe simultaneously a band of width 6 GHz with a 66 kHz resolution, within the 26–40 GHz RF band, have a r.m.s. noise of 7 times the quantum noise limit. The new Q-band HEMT receiver on the Yebes 40-m telescope (**Figure 3**; Tercero et al., 2021) can observe simultaneously 20 GHz, within the 31–50 GHz atmospheric window, with a 38 kHz
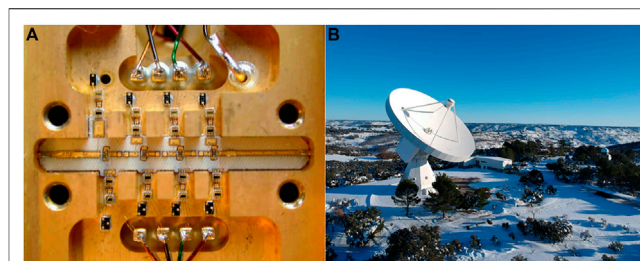

FIGURE 3 | (A) The 4-stage Q-band cryogenic amplifier on the 40-m Yebes telescope (from Tercero et al., 2021). (B) The 40-m Yebes telescope –credit: Pablo deVicente.

resolution and, at frequencies near 40 GHz, a r.m.s. noise around 4 times the quantum limit.

Obviously, the telescope sensitivity also depends on the antenna size, the accuracy of its reflecting surfaces (its aperture efficiency η_A) and the atmosphere transparency. Due to signal absorption by atmospheric water vapour, sensitivity is degraded at shorter radio wavelengths. This is why telescopes operating below 2 mm (i.e., above 150 GHz) are built on high altitude sites. High frequency telescopes must have more accurate surfaces to keep a high aperture efficiency[1]. Large size, high surface accuracy antennas located on high mountain sites are much more difficult to build and need to be protected against harsh weather conditions. In practice, this limits their diameter to about 30 m to operate efficiently at 1 mm wavelength or below.

In order to increase the effective area of a telescope intended to operate at wavelengths shorter than 2 mm, one chooses, rather than increasing the size of a single antenna dish, to build an array of several smaller dishes phased together, i.e., to build an interferometer. Besides cost, a decisive advantage of a phased array of mobile antennas is that its angular resolution can be much better. The latter, which scales with the instrument largest dimension D as λ/D, is a critical parameter in the radio domain.

Another advantage of interferometers vs single-dish telescopes is that they yield spectra with much flatter baselines, as they filter out intensity fluctuations caused by amplifier instabilities and by the Earth atmosphere. This is particularly valuable for the detection of the broad (broadened by Doppler effect) and very weak lines, such as those observed in remote galaxies: As shown in **Section 4.2**, this makes it possible to detect, with proper integration time, molecular lines 10^5 times weaker than the receiver noise throughout a 8 GHz-wide spectrum without removing any baseline. On a spectrum observed with a single dish, one would typically have to remove a high degree polynomial baseline, an operation that may affect the detectability of broad lines.

The interferometers used for the line surveys discussed in the next sections are ATCA, ALMA and NOEMA. ATCA is an array of 6 × 22-m diameter antennas operating down to 7-mm

---

[1]Aperture efficiency, η_A, according to Ruze's equation, scales with the r.m.s. surface error ϵ as $\exp(-(4\pi\epsilon/\lambda)^2)$, which means that ϵ must be $\leq 50\mu m$ to achieve an efficiency $\eta_A \geq 0.5$ at a wavelength $\lambda \leq 1$ mm.
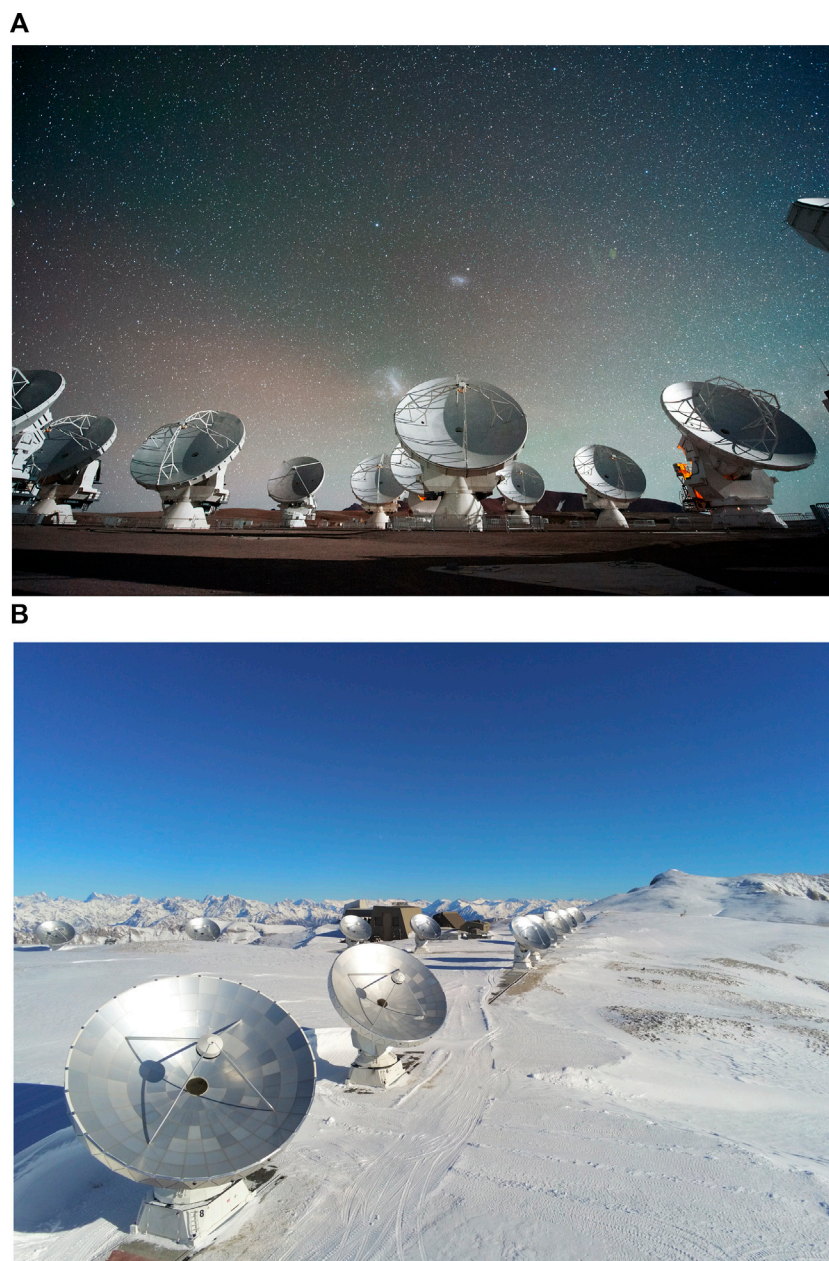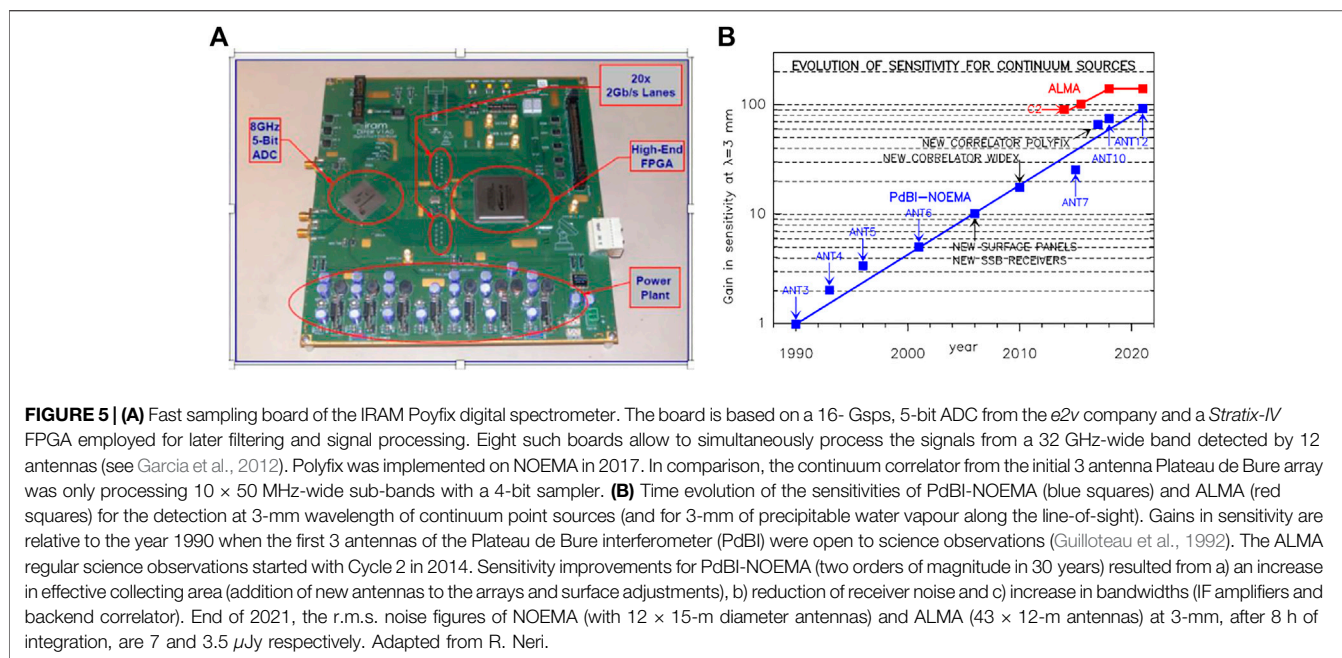
FIGURE 4 | (A) Night view of the ALMA 12-m antenna array on the Chajnantor Plateau in the Chilean Andes at 5,000 m altitude. The Magellanic Clouds appera as two white cloudlets in the night sky –credit: ESO.org. **(B)** The NOEMA interferometer, operating on the Plateau de Bure in the Alps at 2,550 m altitude. Credit: J. Boissier, IRAM.

wavelength (50 GHz) and located at 240 m altitude, $-30°$ latitude, in New South Wales, Australia. The ALMA 12-m array consists of an array of 50 high accuracy, 12-m diameter parabolic antennas, located at 5,000 m altitude, $-23°$ latitude, in the Atacama desert in Chile. It operates down to 0.3 mm wavelength (950 GHz) thanks to the low water vapour content of the atmosphere above the site. This 12-m array is seconded by a smaller array of twelve 7-m antennas plus four 12-m antennas, ACA, also known as the Morito-san array (**Figure 4A**). Finally, NOEMA was upgraded end of 2021 to

a 12×15-m diameter antenna array; it is located on a 2,550 m altitude plateau in the southern Alps in France and operates down to 1 mm wavelength with 12 antennas (and currently 0.8 mm, or 375 GHz, with six antennas). NOEMA is the largest mm-wave array in the Northern Hemisphere (**Figure 4B**). Its SIS junction receivers and its wide band XF Fast Fourier Transform correlator make it particularly well suited for extragalactic spectral surveys, since it can instantaneously cover a 32 GHz-wide bandwidth with 2 MHz-wide (2.6 kms^{-1} at 230 GHz) spectral channels (see **Figure 5**).

FIGURE 5 | (A) Fast sampling board of the IRAM Poyfix digital spectrometer. The board is based on a 16- Gsps, 5-bit ADC from the *e2v* company and a *Stratix-IV* FPGA employed for later filtering and signal processing. Eight such boards allow to simultaneously process the signals from a 32 GHz-wide band detected by 12 antennas (see Garcia et al., 2012). Polyfix was implemented on NOEMA in 2017. In comparison, the continuum correlator from the initial 3 antenna Plateau de Bure array was only processing 10×50 MHz-wide sub-bands with a 4-bit sampler. **(B)** Time evolution of the sensitivities of PdBI-NOEMA (blue squares) and ALMA (red squares) for the detection at 3-mm wavelength of continuum point sources (and for 3-mm of precipitable water vapour along the line-of-sight). Gains in sensitivity are relative to the year 1990 when the first 3 antennas of the Plateau de Bure interferometer (PdBI) were open to science observations (Guilloteau et al., 1992). The ALMA regular science observations started with Cycle 2 in 2014. Sensitivity improvements for PdBI-NOEMA (two orders of magnitude in 30 years) resulted from a) an increase in effective collecting area (addition of new antennas to the arrays and surface adjustments), b) reduction of receiver noise and c) increase in bandwidths (IF amplifiers and backend correlator). End of 2021, the r.m.s. noise figures of NOEMA (with 12×15-m diameter antennas) and ALMA (43×12-m antennas) at 3-mm, after 8 h of integration, are 7 and 3.5 μJy respectively. Adapted from R. Neri.

3 COMPLEX ORGANIC MOLECULES IN THE DARK CLOUD TMC-1

Cold dark clouds have turned up to be amazingly rich chemical laboratories, able to synthesize *in situ* a great variety of molecules. Most of the identified species are neutral molecules, although several cations, essentially protonated forms of abundant closed-shell species (Agúndez et al., 2015a, Marcelino et al., 2020, Cernicharo et al., 2020a; Cernicharo et al., 2021a; Cernicharo et al., 2021b), but also a few hydrocarbon and nitrile anions, have also been observed (Cernicharo et al., 2020b). Molecular ions have low abundances, typically below 10^{-10} relative to H_2, due to their high reactivity.

TMC-1 is a cold pre-stellar core located within Heiles' Cloud 2 in the Taurus constellation (Cernicharo and Guélin, 1987). Target of very many studies (Fuente et al., 2019, and references therein) it was early on recognized as a rich molecular source. Within the Taurus cloud complex, several dark cores present similar physical characteristics (Cernicharo et al., 1984), but TMC-1 stands out as the one where the largest amount of carbon-bearing molecular species has been detected.

TMC-1 presents an interesting carbon-rich chemistry that leads to the formation of long carbon-chains, radicals, ions and neutral closed-shell molecules such as cyanopolyynes (Cernicharo et al., 2020b; Cernicharo et al., 2020c and references therein). This cold dark core also hosts a number of nearly saturated species, such as CH_3CHCH_2, more typical of hot star-forming cores (Marcelino et al., 2007). A first polar benzenic ring, benzonitrile C_6H_5CN, has been detected in this object (McGuire et al., 2018), although benzene itself is only observed in post-AGB star envelopes. In spite of this carbon-dominated chemistry, a number of carbon chains containing oxygen have been detected in TMC-1: CCO (Ohishi et al., 1991), C_3O (Matthews et al., 1984), HC_3O^+ (Cernicharo et al., 2020a),

HC_3O and C_5O (Cernicharo et al., 2021k) HC_5O, and HC_7O (Cordiner et al., 2017; McGuire et al., 2017; Cernicharo et al., 2021k). The path leading to the formation of HC_5O and HC_7O remains a mystery (Cernicharo et al., 2021k), all the more that the related chains C_4O, HC_4O, and HC_6O have not been found (HC_2O is netherless observed in other cold dense clouds—Agúndez et al., 2015b). Other O-bearing species, more typical of hot cores and corinos, such as CH_3OH, C_2H_3CHO, C_2H_3OH, $HCOOCH_3$ and CH_3OCH_3, have also been identified in TMC-1 mm-wave spectra (Agúndez et al., 2021a).

Since Léger and Puget's assertion (Léger and Puget, 1984; Allamandola et al., 1985) that the carriers of the unidentified infrared bands must be polycyclic aromatic hydrocarbons (PAHs), efforts have been devoted to understand how those species may form in space. Cherchneff et al. (1992) proposed that the envelopes surrounding carbon-rich AGB stars could be PAH factories. Along this line, the detection of benzene in the C-rich protoplanetary nebula CRL 618 (Cernicharo et al., 2001) suggested a bottom-up approach in which the small hydrocarbons formed during the AGB phase, such as C_2H_2 and C_2H_4, interact with the ultraviolet (UV) radiation emitted by the star when it evolves towards a white dwarf (Woods et al., 2002; Cernicharo 2004). Alternately, in a top-down approach, PAHs would result from the stripping of graphite grain surfaces chemically processed or irradiated by stellar UV (Pilleri et al., 2015; Martínez et al., 2020). Hence, it is startling to discover that a cold dark cloud, shielded from UV and devoid of internal energy sources, hosts not only very long C-chain molecules such as HC_9N, but also C-cycles and aromatic rings.

This exciting result mainly stems from two on-going line surveys of TMC-1 between 20 and 50 GHz: GOTHAM (**G**BT **O**bservations of **T**MC-1: **H**unting **A**romatic **M**olecules; McGuire et al., 2018) and QUIJOTE (**Q**-band **U**ltrasensitive **I**nspection **J**ourney in the **O**bscure **TMC-1** **E**nvironment; Cernicharo et al.,
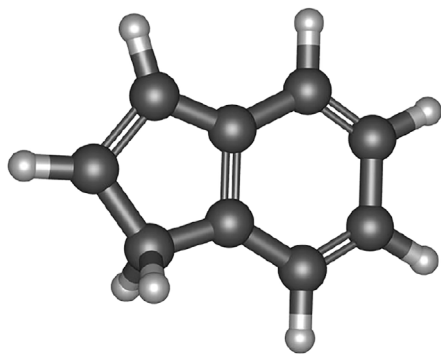
FIGURE 6 | Indene structure (from Cernicharo et al., 2021d).

2021c). Both surveys follow the pioneering work of Kaifu et al. (2004), who first surveyed the whole 8.8–50 GHz frequency spectrum in that source with the Nobeyama 45-m telescope. N. Kaifu, S. Saito and their colleagues identified in the surveyed band 414 lines pertaining to 38 molecular species. The Nobeyama survey data were subsequently used by McGuire et al. (2018) to find, through spectral stacking, a hint of the presence of benzonitrile, a presence superbly confirmed by the GOTHAM survey.

The GOTHAM and QUIJOTE surveys represent a major leap in sensitivity with respect to previous works. They use the 100-m diameter GBT and the recently completed 40-m Yebes radio telescope, that benefit from higher effective areas and, mostly, from lower noise and broader bandwidth receivers. The teams of both surveys reported the detection of several cyclic molecules. The GOTHAM team mostly used a spectral stacking technique (consisting, for a given polar molecule, in a weighted average of the very many rotational transitions covered by the survey) to achieve their detections. The QUIJOTE team, owing to the higher (sub milli-kelvin) sensitivity of its survey, was able to detect individual lines without the need to rely on blind line stacking (**Figure 7**). Among the QUIJOTE detections, we stress those of indene, the first double-cycle detected in space (**Figures 6**, 7 and Cernicharo et al., 2021c; see also Burkhardt et al., 2021), of cyclopentadiene (Cernicharo et al., 2021d), and *ortho*-benzyne (Cernicharo et al., 2021c). Detections reported by the GOTHAM and QUIJOTE teams include ethynyl and cyano derivatives of cyclopentadiene, benzene, and naphthalene (McCarthy et al., 2021; Lee et al., 2021; Cernicharo et al., 2021f; Cernicharo et al., 2021j).

It is unlikely that such complex molecules and cycles arose from a reservoir pre-existing to the formation of the TMC-1 core: they could have hardly survived in the diffuse gas transparent to UV radiation. McGuire et al. (2021) propose a reasonable chemical network starting with the phenyl radical that may explain the observed abundances of cyanonaphthalene, but the chemical routes leading to this radical and benzene itself remain unclear. An *in situ* formation mechanism for benzene must involve abundant hydrocarbons containing from 2 to 4 carbon atoms. Moreover, those hydrocarbons should react and form C-rings in a mere 2 or 3 steps to be able to form enough benzene or phenyl radicals (Joblin and Cernicharo, 2018).

The propargyl radical, CH_2CCH, has recently been found in TMC-1 by Agúndez et al. (2021b) with an abundance close to 10^{-8} relative to H_2. In addition, complex hydrocarbons such as vinyl and allenyl acetylene have also been observed with fairly large abundances (Cernicharo et al., 2021e; Cernicharo et al., 2021f). These hydrocarbons may hold the key to form the first aromatic rings, from which larger PAHs can grow. In two recent articles reporting the detections of *ortho*-benzyne and the ethynyl derivatives of cyclopentadiene (Cernicharo et al., 2021c; Cernicharo et al., 2021g), the authors reproduce reasonably well the observed abundances of C-cycles with reactions between the radicals CH, CCH, C_4H, CH_2, ... and the C-chains CH_3CCH, H_2CCCH, CH_2CHCCH, and $H_2CCCHCCH$ (see **Figure 8**). This requires, however, to reduce the abundance of oxygen to a level close to that of carbon: the presence of free oxygen atoms, which efficiently react with the hydrocarbons, would strongly reduce the yield of five or six C-atoms rings, hence impede the formation of PAHs. A similar result was reported for other species by Fuente et al. (2019).

In addition to hydrocarbons (closed shells and radicals) and their cyano and ethynyl derivatives, TMC-1 revealed itself as an efficient sulfur factory, through the identification of a number of complex sulfur-bearing species in the QUIJOTE survey: HC_3S^+, HCCS, NCS, H_2CCS, H_2CCCS, C_4S, HCSCN, and HCSCCH (Cernicharo et al., 2021h; Cernicharo et al., 2021i).

Most remarkably, in just a couple of years, The GOTHAM and QUIJOTE surveys have increased the number of known interstellar molecules from 204 to 256 and revealed the great potential of TMC-1 for further investigations.

4 MOLECULES IN THE DISTANT UNIVERSE

How much can we learn about the interstellar gas in nearby galaxies and farther out, in the remote parts of the Universe? Observing increasingly distant sources means travelling back in time. Because the Universe is expanding, the radiation emitted by distant sources (and the spectral lines it may contain, e.g., Lyα, CII and MgII lines) appears to us redshifted. Models of the Universe expansion tell us the relation between redshift and distance. Except for the 2.7 K Cosmic Background, the remotest sources we can observe are the very first quasars, the bright radio/infrared quasi-stellar sources that appeared at the center of the primordial galaxies during the epoch of reionization, some 700 million years after the Big Bang. The most distant quasar identified as of today, J0313–1806, has a redshift $z \simeq 7.64$ when the Universe was only 680 million light-years old (Wang et al., 2021).

Whereas the lines observed in optical spectra teach us about these remote quasi-stellar objects' redshift, age and elemental composition, they are far too broad to inform us on the dynamics of the emitting gas (e.g., Wildy and Czerny 2017) and, mostly, on its molecular and isotopic compositions. Those latter can only be studied at sub-millimeter and millimeter
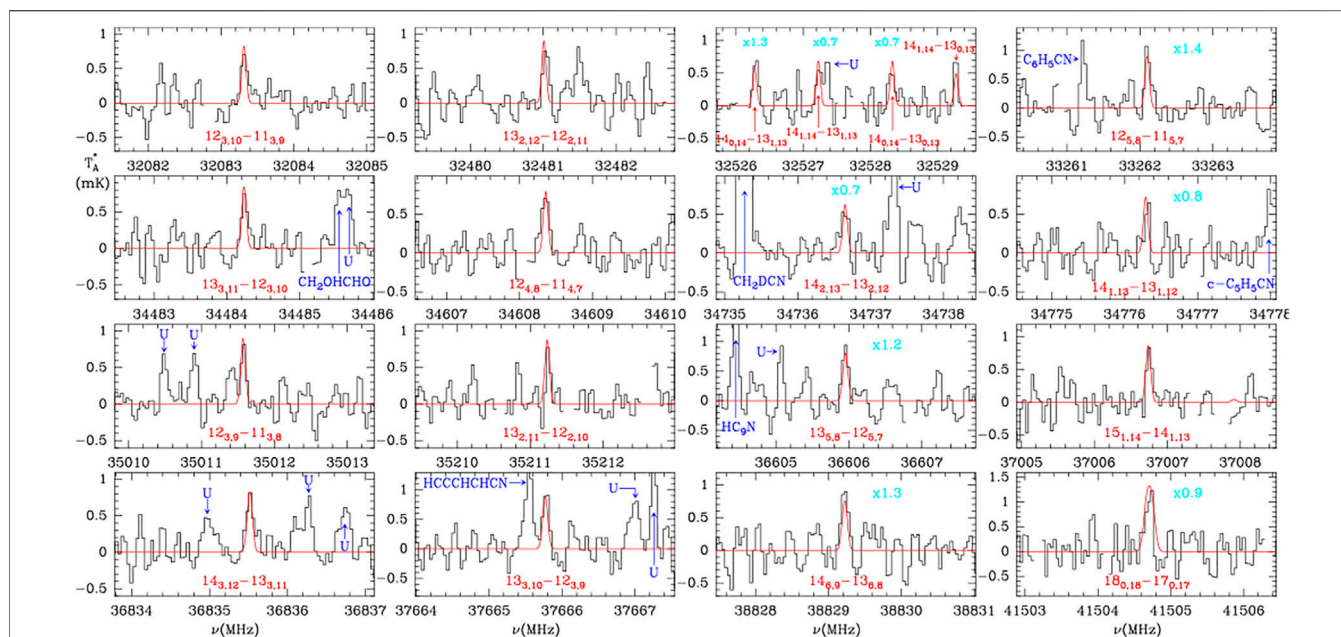
FIGURE 7 | Indene transitions observed towards TMC-1 with the Yebes 40-m radio telescope by Cernicharo et al., 2021d.
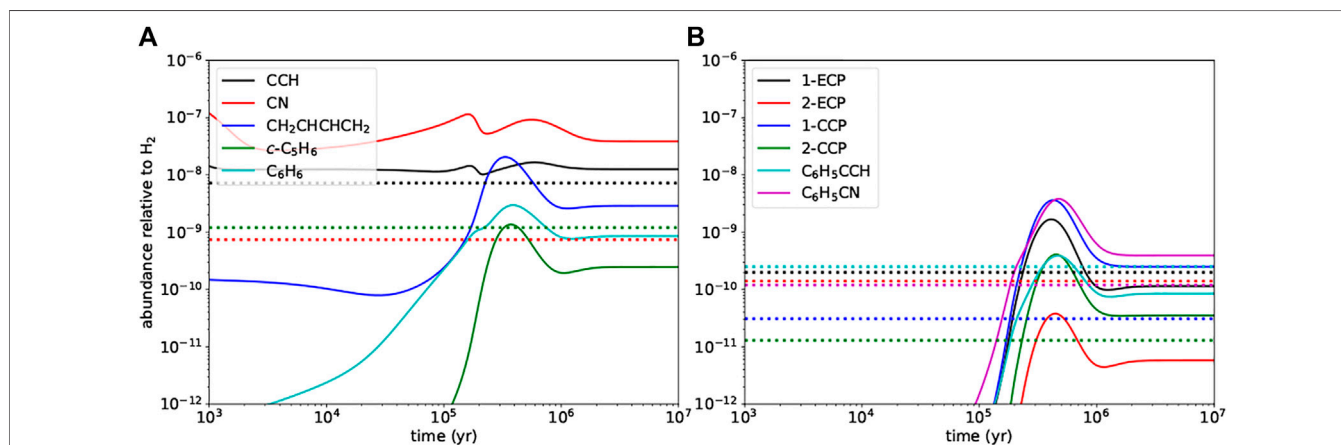

FIGURE 8 | Calculated abundances of CCH and CN derivatives of c-C_5H_6 and C_6H_6 **(B)** and of their precursors **(A)**. The horizontal dotted lines correspond to the abundances observed in TMC-1. The species 1/2-ECP correspond to two isomers of ethynyl cyclopentadiene, while the species 1/2-CCP correspond to two isomers of cyano cyclopentadiene (from Cernicharo et al., 2020g).

wavelengths, preferably in circumstances that compensate for the extreme line weakness.

The most favourable case is when the line-of-sight to the remote quasar is intercepted at halfway by a massive galaxy or a cluster of galaxies (halfway is the optimum distance for a magnification of the quasar radiation by gravitational lensing). If the quasar is radio-loud, the gas of the intervening galaxy may absorb the quasar continuum radiation, causing the rotational line pattern of the polar molecules to appear in absorption against the magnified background continuum. The gas disks of galaxies are thin, so that the absorption lines are fairly narrow and their carriers can be unambiously identified. On the same mm spectrum, but at longer

wavelengths (i.e., at higher redshift), one may detect in emission, magnified by the lens, molecular lines arising in the quasar itself.

The Planck/HIFI, Hershell/HerMES, H-ATLAS and South Pole Telescope far-infrared/sub-millimetre surveys show that a fair fraction (several percent) of the high-z sub-millimetre-bright galaxies are magnified by gravitational lensing (Ade et al., 2016; Spilker et al., 2016, as well as references therein; Hodge and da Cunha, 2020). Nonetheless, and except for the relatively strong CO and H_2O lines (Yang et al., 2016; Pensabene et al., 2021), rare are the cases where the magnification is large enough to allow a clear detection of molecular lines from the intervening galaxies, or from the background quasar itself.

Besides the detections in a handful of lensed quasars (e.g., APM08279+5255) of a few lines of HCN, HNC and HCO$^+$ (García-Burillo et al., 2006; Guélin et al., 2007), one has essentially to rely on source stacking methods to barely detect more molecular species (Spilker et al., 2014; Reuter et al., 2020). A couple of sources, however, are lucky exceptions: a field galaxy on the line-of-sight to the bright radio-loud quasar PKS1830-211, and a strongly lensed quasi-stellar object, H1413+117, dubbed *the Cloverleaf*. We now focus on those two remarkable objects.

4.1 Molecules Inside an Arm of a Spiral Galaxy at Redshift z = 0.89

With a continuum flux of 2–3 janskys at 3-mm, the quasar PKS 1830–211 (redshift $z = 2.5$, Lidman et al., 1999) is the brightest lensed source at millimetre wavelengths. Its line-of-sight is intercepted by two galaxies: the nearest to us is responsible for HI absorption at redshift $z = 0.19$; the other, which appears on HST images as a face-on spiral galaxy, gives rise to HI and molecular line absorption at $z = 0.89$ (e.g., Muller et al., 2006; Combes et al., 2021). The galaxy acts as gravitational lens that splits the quasar image into two compact radio images, respectively located $0.6''$ NE and $0.4''$ ($\simeq$ 6 kilo light-years) SW of the galaxy center. The compact SW radio image lies just behind a spiral arm visible on the I-band HST image (**Figure 9A**).

The millimeter wave spectrum observed along both NE and SW lines-of-sight displays a dense pattern of absorption lines. The SW one is particularly rich and not unlike those observed in the arms intercepting the line-of-sight to the HII region SgrB2, close to the Milky-Way center, or those inside the central starburst of the nearby Sc spiral galaxy NGC 253 (Martin et al., 2006). A detailed analysis of the line intensities and profiles, as well as of the chemistry of their carrier molecules, allows us to estimate the physical conditions and morphology of the clouds intercepting both lines-of-sight (Muller and Guélin, 2008; Muller et al., 2014). The SW line-of-sight crosses a number of mostly cold (≤ 40 K) relatively dense clouds ($n_{H_2} \geq 10^4$ H$_2$ molecules per cm^3), surrounded by a diffuse envelope. The NE one encounters only diffuse clouds ($n_{H_2} \leq 10^3$ cm^{-3}) transparent to stellar UV radiation.

A total of 54 molecular species (not counting isotopologues) have been identified in the parts of the spectrum surveyed to date: a 20 GHz-wide band at 7-mm wavelength with the ATCA interferometer and the Yebes 40-m telescope, a 8 GHz-wide band at 3-mm with NOEMA, and a 38 GHz-wide band between 3-mm and 0.6-mm with ALMA (Muller et al., 2011; Muller et al., 2014; Muller et al., 2016; Muller et al., 2017) and references therein (Muller et al., 2020; Tercero et al., 2020).

These species are light hydrides (HF, CH, CH$^+$, CH$_3^+$, ND, NH$_2$, NH$_3$...), small hydrocarbons (CCH, C$_3$H, C$_4$H, C$_3$H$^+$, H$_2$CN, C$_3$N, ...), sulfur-bearing species (SH$^+$, SO, SO$_2$, NS...) but also heavier, more complex organic molecules with up to seven atoms (see **Figure 9**): aldehydes (formaldehyde and thioformaldehyde, acetaldehyde CH$_3$CHO), imines (CH$_2$NH methanimine), amines (CH$_3$NH$_2$ methylamine), cyanides (CH$_2$CHCN, vinyl cyanide), amides (formamide NH$_2$CHO, urea (NH$_2$)$_2$CO), one alcohol (methanol CH$_3$OH), and its thioalcohol (CH$_3$SH, methyl mercaptan), and one

organic acid (formic acid HCOOH). Their detection suggests that all the ingredients necessary for a rich prebiotic chemistry are present in the gas, although the physical conditions (density, temperature) necessary for starting such a chemistry are ways from being fulfilled even in the dense and hot prestellar cloud cores. Nevertheless, the chemical composition of the gas in this distant object is not very different from that of interstellar clouds in the Milky-Way.

The basic ingredients of Miller-Urey experiment (H$_2$, H$_2$O, CH$_4$ and NH$_3$) and of closely related experiments (CO, CO$_2$, H$_2$S, SO$_2$) are all present there (the nonpolar species H$_2$, CH$_4$ and CO$_2$ cannot be observed in the radio domain). Also present are some emblematic intermediate products of these experiments: hydrogen cyanide and isocyanide, formaldehyde, urea, acetylene, cyanoacetylene, formic acid and, mostly, formamide the key to the peptide bond. As shown by the experimental work and ab-initio calculations reported by Ferus et al. (2018), formamide is a possible source for the synthesis of amino acids and of the four RNA nucleobases (uracil, cytosine, adenine and guanine).

4.2 Molecules in a Young Quasar at Redshift z = 2.6

The Cloverleaf Quasar (H1413+117) is the archetype of gravitationally lensed quasars and one of the most luminous and best studied objects in the distant, hence young Universe. The quasar redshift ($z = 2.557\,86$) implies a distance of 11 billion light-years from the Sun and an age of about 2 Gyr after the appearance of the very first stars, 700 million years after the Big Bang. Located at the center of a starburst galaxy, its radiation, viewed from the Earth, is magnified by a factor as large as 11 (according to models of Kneib et al., 1998; Venturini and Solomon, 2003) by 2 galaxies, with redshifts z $\simeq$ 1 and 2, respectively, that intercept the line-of-sight and split the quasar image into 4 distinct components **Figure 10**).

The Cloverleaf quasar and its host galaxy have been studied in the X-ray, optical and radio domains, and more particularly at sub-millimetre wavelengths in the continuum and the lines of CO and HCN. The far infrared/sub-millimetre emission appears to arise from an extended (3 light-year radius) disk of gas and dust rotating around the active galactic nucleus (or AGN—Alloin et al., 1997; Barvainis et al., 1997; Solomon et al., 2003; Bradford et al., 2009).

The molecular emission is currently the object of high sensitivity line surveys using NOEMA and ALMA. Thirty four molecular lines pertaining to fourteen molecular species are identified within the (still partly) surveyed 200 GHz-wide frequency band covering the rest frequency ranges: 338–365, 526–626 and 705–786 GHz. (**Figures 11**, **12**). Some of those lines correspond to different rotational transitions of the same species, such as the J $\rightarrow$ J' = 1-0, 4-3, 6-5, 7-6, and 8-7 transitions of HCN and HCO$^+$, the 4-3, 6-5, 8-7 transitions of HNC, the 1-0, 3-2, 4-3, 6-5, 8-7, 9-8 transitions of ^{12}CO, the main isotopologue of CO, as well as the 5-4 and 7-6 transitions of the rare isotopologues ^{13}CO and C^{18}O.

The detected lines sample a wide range of energy levels and opacities for a given molecule, and different excitation conditions for molecules that are believed to be coeval. From
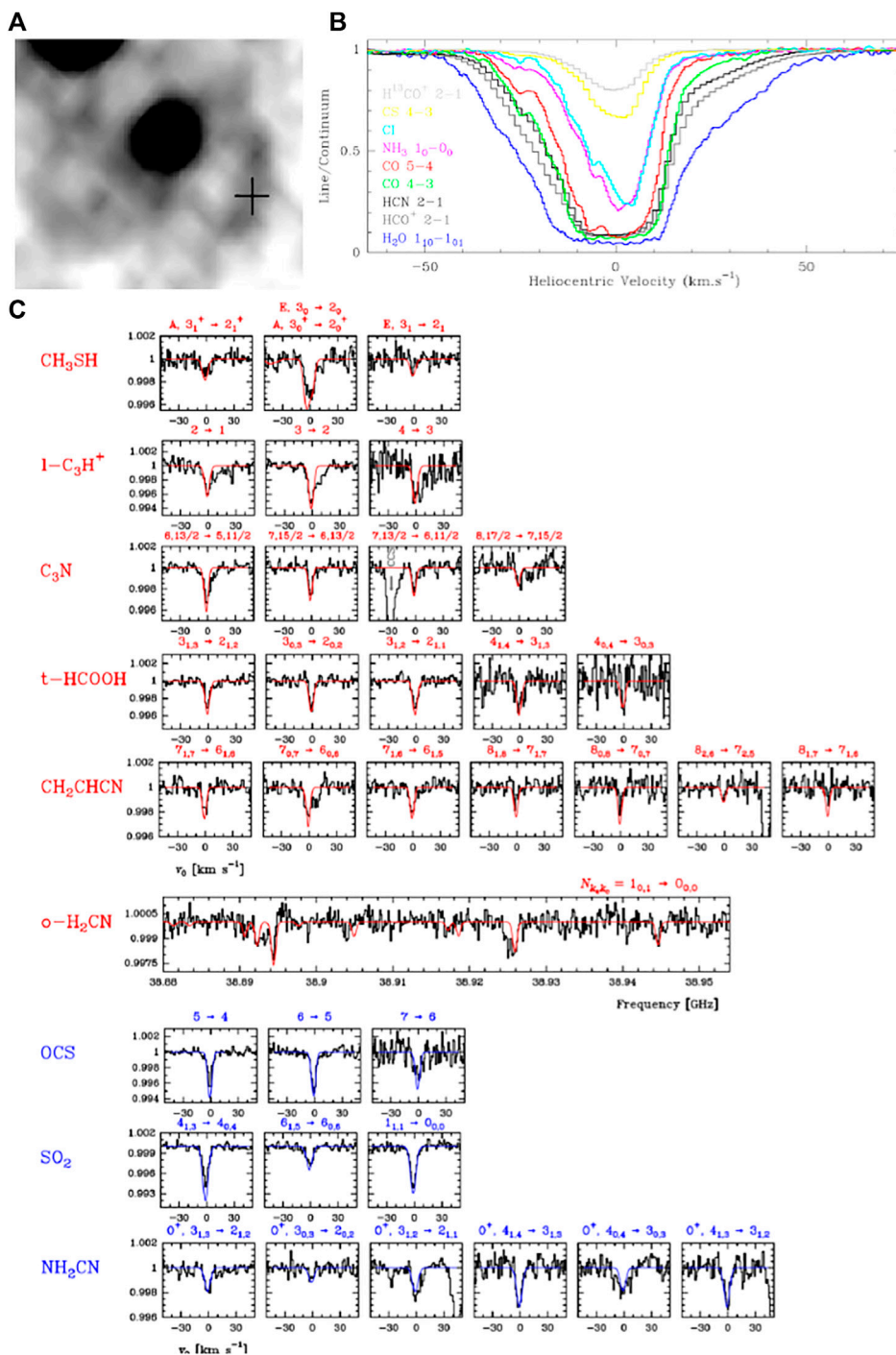
FIGURE 9 | (A): The spiral galaxy at $z = 0.89$ intercepting the line of sight to the quasar PKS 1830–211, as seen by the Hubble satellite in the I band (Winn et al., 2002). The cross shows the position where the molecular lines are observed in absorption in the SW spiral arm. **(B)**: Profiles of the strongest absorption lines observed by ALMA in the SW arm (Muller et al., 2014). Abscissa is the gas velocity in the source frame (i.e., after correction for the redshift of the source $z = 0.885\,875$). Ordinate is the line to continuum ratio, where the continuum arises from the SW image of the background quasar. **(C)**: Absorption lines observed toward the SW arm with the Yebes 40-m telescope. The species identified for the first time in an extragalactic source are highlighted in red. The molecules highlighted in blue are those that were identified for the first time in this source, but observed previously in other extragalactic sources. The y-axis is the normalised intensity to the total (NE + SW) continuum level (from Tercero et al., 2020).
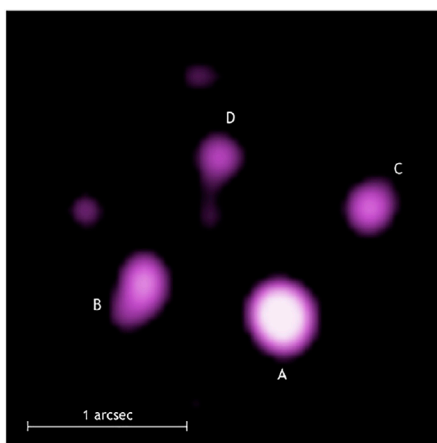
FIGURE 10 | The Cloverleaf Quasar, Chandra Xray image. Credit: NASA.

the TMC-1 Galactic cloud, but similar to that in the HII region SgrB2 (Weiss et al., 2013). Its intensity is however far more intense than in any Galactic source, implying an exceptionally strong starburst: the mass of very dense gas is estimated to be at least 10^{10} Solar masses and the star formation rate $\dot{M} = 10^3$ Solar Masses per year (Stacey et al., 2021). This is 200 times larger than the star forming rate in the entire Milky-Way and comparable to those of the brightest ultra luminous infrared galaxies, or ULIRGs. (Solomon et al., 2003; Robintaille and Whitney, 2010).

In contrast to the absorption spectra observed toward PKS1830-211, where the line intensities primarily depend on the background quasar continuum flux, the lines detected in emission in a remote radio-quiet object like the Cloverleaf depend on its distance and are therefore very weak. No wonder that most of the molecules observed there are di- or triatomic species. Some are radicals and ions (CH, CCH, H_2O^+) characteristic of gas irradiated by stellar UV, i.e. of diffuse clouds. The others (CO, CS, HCN, HNC, HCO^+ H_2O, H_2S) are stable species belonging to UV-shielded clouds. Remarkably, these stable species are the same as the very first identified in Galactic clouds 50 years ago, when the sensitivity of mm-wave radio telescopes precluded to detect more than a dozen of molecular lines.

As much as we can tell from the line intensities in **Figures 11**, **12**, the abundances of HCN and HCO^+, relative to the abundance of CO (the best tracer of the molecular gas), are similar in the Cloverleaf Quasar ($1 - 3 \times 10^{-3}$) to those in the $z = 0.89$ spiral galaxy and in the nearby Galactic cloud TMC-1
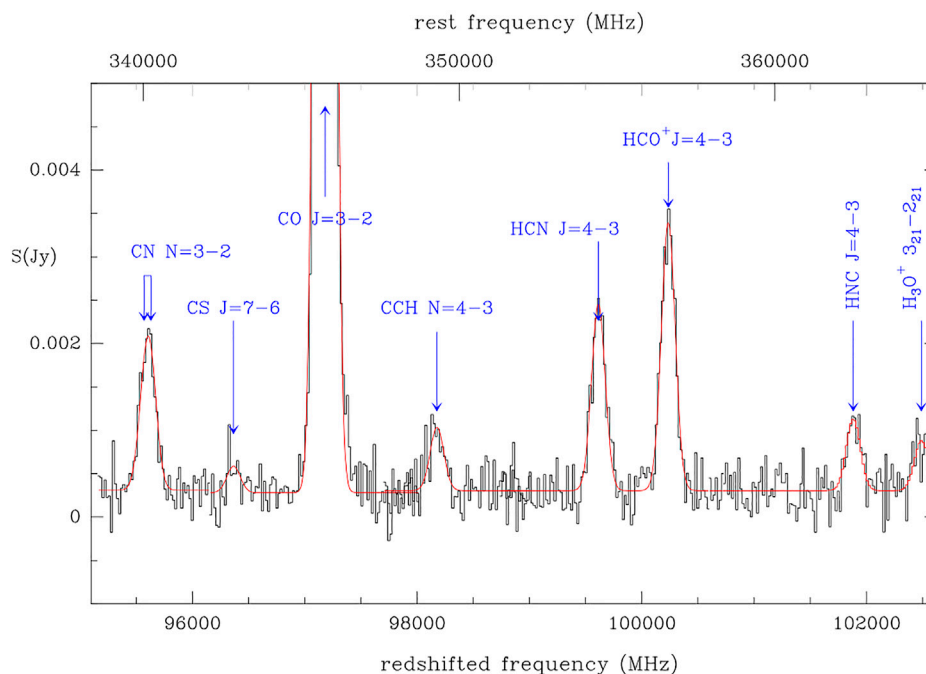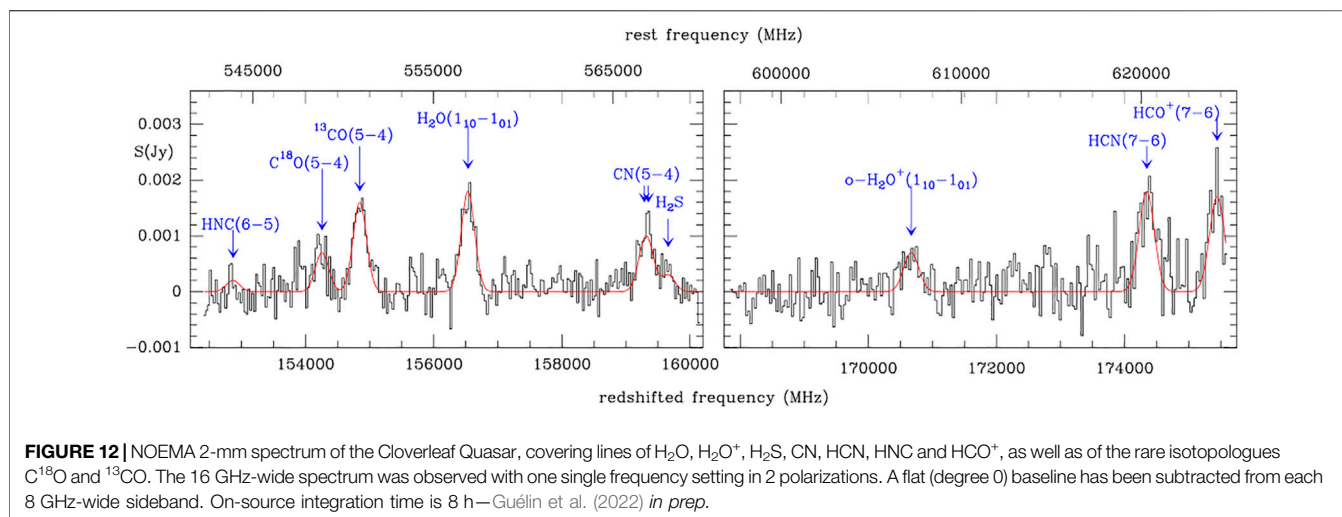
this, and from the spectral energy distribution of the quasar continuum emission, it is possible to assess the density, temperature and radiation field in the emitting region, as well as the molecular abundances. The constancy of the line width (half-power width $440\,\mathrm{km s^{-1}}$) seems to imply that the molecules are distributed throughout the same rotating cloud complex.

Besides the AGN emission, the far infrared radiation field is mainly thermal emission from tiny dust grains with temperatures in the range 30–100 K, i.e., warm compared to

FIGURE 11 | ALMA 3-mm spectrum of the Cloverleaf Quasar covering the N/J = 3-2 lines of CN and CO, and the J = 4-3 lines of HCN and HCO⁺. Ordinate scale is line flux in janskys. Abcissa is observed frequency in MHz. Upper scale is rest frequency in the quasar frame. On-source integration time is 14 h. —Guélin et al. (2022) in prep.

FIGURE 12 | NOEMA 2-mm spectrum of the Cloverleaf Quasar, covering lines of H_2O, H_2O^+, H_2S, CN, HCN, HNC and HCO^+, as well as of the rare isotopologues $C^{18}O$ and ^{13}CO. The 16 GHz-wide spectrum was observed with one single frequency setting in 2 polarizations. A flat (degree 0) baseline has been subtracted from each 8 GHz-wide sideband. On-source integration time is 8 h—Guélin et al. (2022) *in prep.*

(Muller et al., 2011), hence in an extremely wide range of environments and at all Cosmic ages greater than 1 Gyr. We note that the $^{13}CO/C^{18}O$ isotopic abundance ratio on **Figure 12**, 2.5, is typical of nearby star-forming galaxies and significantly larger than the values $\simeq 1$ reported by Zhang et al. (2018) for dust-enshrouded starbursts at similar redshift.

Water vapour is detected and fairly abundant in all those objects. It seems ubiquitous in remote quasars (Yang et al., 2016; Yang et al., 2019; Yang et al., 2020), as it is in all Milky-Way molecular sources, where it is observed in both forms, gaseous and solid. The H_2O submillimetre rotational lines, are typically the strongest after those of CO. The H_2O and CO lines have similar profiles, which seems to imply both molecular species are coeval.

5 CONCLUSION AND PROSPECTS

We do know, from the spectral analysis of stellar light and meteorites, that the elemental composition of matter is similar throughout the Universe, at least as concerns the most abundant elements: H, He, O, C, N, Ne, Si, Mg, S, P, and Fe . . . It basically follows the nuclear binding energies and, in the case of peculiar stars, depends on their mass, which governs nucleosynthesis.

Things, of course, are less straightforward as concerns the gas molecular composition, in view of the extraordinary large range of physical and enviromental conditions prevailing in IS space. It was thought, for a long time, that the harsh conditions (typically densities below few hundreds atoms per cubic cm, gas temperature of few tens of kelvin, stellar and cosmic-ray induced UV radiation) preclude the survival of any molecule, but for a few ephemeral diatomic species like the already identified CH, CH^+ and CN. That view was overturned at the end of the 1960s when it was realized that shielding by dust grains and H atoms, and self-shielding of H_2, N_2 and CO molecules, considerably reduce the photodestruction of those and very many other molecular species in IS clouds. And indeed, in the following

years formaldehyde, H_2CO and CO were not only detected, but observed in about every dark or bright IS nebula. In the course of years, owing to remarkable gains in sensitivity and angular resolution of the mm-wave and far-IR telescopes, the list of molecules identified in interstellar and circumstellar clouds has steadily increased to reach 256 species [see Mc Guire (2018) for a list of molecules identified until 2018 and *The Astrochymist*[2] for a monthly update of that list.]

Most remarkably, HCN and H_2O are found to be ubiquitous in clouds shielded by dust from stellar UV radiation. As we have seen, they are observed up to the edges of the Universe. Quite sensitive to stellar UV and cosmic-ray induced photodestruction, these species cannot survive for a very long time even in the densest clouds, hence have to be renewed on relatively short timescales in a variety of environments. HCN is a prerequisite brick for the formation of polymers via peptide bonds, whereas liquid H_2O, a solvent of polar molecules, is essential in shaping up complex molecular structures. Their omnipresence in the gas or on dust grains opens the way to organic molecules: formaldehyde, formamide, methanol, ethanol, urea . . .

Along this line, the recent gains in sensitivity, allowed by the new generation radio telescopes, brought an unexpected result: the identification in the quiescent dark cloud TMC-1 of fairly complex organic compounds, linear chains or cycles, consisting of six or more C-atoms. Latest examples are benzyne (c-C_6H_4), indene (c-C_9H_8 –**Figures 6, 7**) and cyanoethyleneallene ($H_2C_2CHC_3N$; Shingledecker et al., 2021) that were discovered this year together with a score of new hydrocarbons or cyanohydrocarbons (the attachment of a CN radical increases the polarity of hydrocarbons, easing their radio detection). Yet, TMC-1 would seem to be the last place where complex molecules would form: its relatively short age (few x 10^5 years) coupled to a vanishingly low gas density (few x 10^4 H_2 molecules per cm^3), extremely low gas temperature ($T_k \simeq 10$ K), and to a total lack of

---

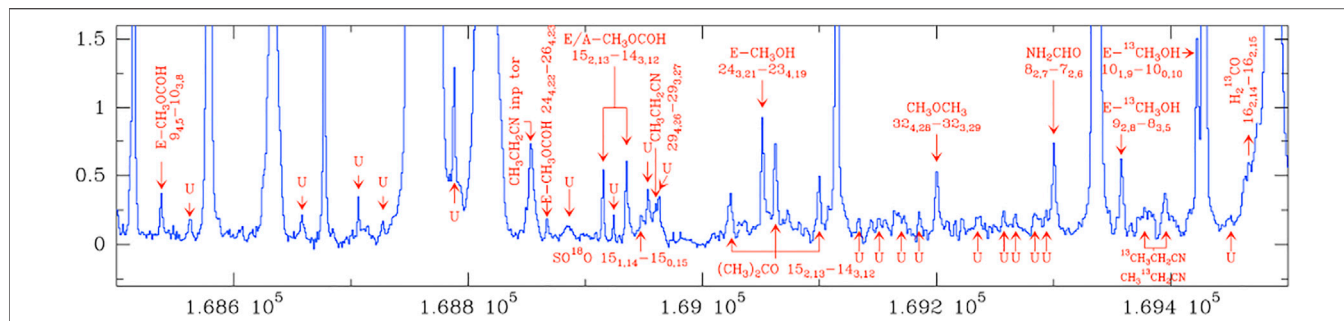[2]The Astrochymist avalaible at: http://www.astrochymist.org/.

FIGURE 13 | 1 GHz-wide portion of the sub-millimeter spectrum of the Orion-KL star-forming cloud at 2 mm. The spectrum, which is part of an extended (80–281 GHz) spectral survey made with the IRAM 30-m radio telescope, is confusion-limited above 200 GHz (Tercero et al., 2010).
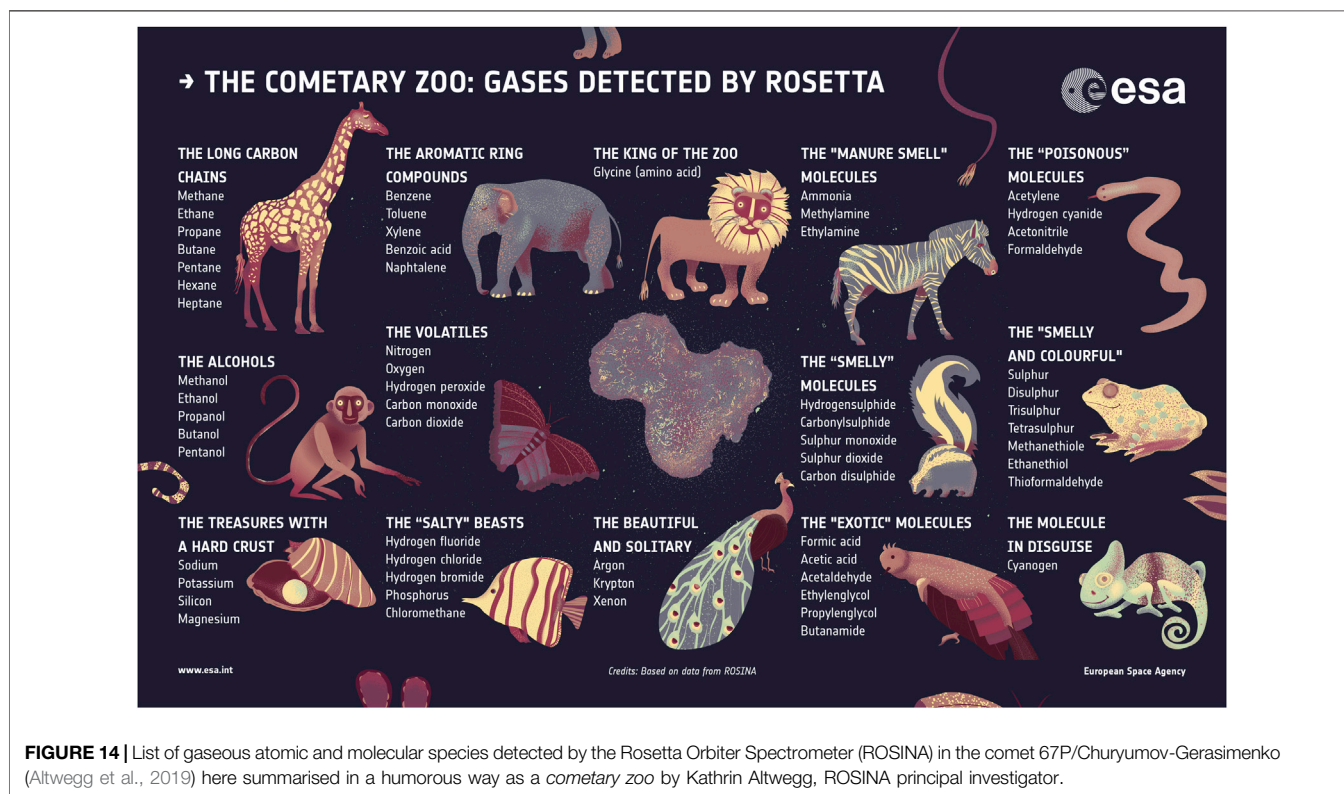

FIGURE 14 | List of gaseous atomic and molecular species detected by the Rosetta Orbiter Spectrometer (ROSINA) in the comet 67P/Churyumov-Gerasimenko (Altwegg et al., 2019) here summarised in a humorous way as a *cometary zoo* by Kathrin Altwegg, ROSINA principal investigator.

internal or nearby energy sources, should have made molecule formation a formidable challenge.

The list of molecules identified in TMC-1 has more than doubled in the last 2 years, even though, due to the very low temperature, most of the oxygen atoms are frozen on the dust grains in the form of water and dry ices, or trapped into CO molecules. For sure, many more will be discovered as low frequency searches for heavy organic molecules intensify. In warmer and denser sources, such as star-forming clouds and Giant Molecular clouds (OrionA-KL, SgrB2-N, ...), not only reactions in the gas phase do proceed faster, but also the molecules formed on the grains may sublimate. Their molecular content is obviously richer than that of the cold dark clouds, especially as concerns complex organic compounds. The census

of those, however, becomes more challenging, as the gas is more turbulent in such sources and the molecular lines are broader, so that the mm-wave (and far-IR) spectra reach much sooner the confusion limit (**Figure 13**). Prospects are more favourable for Protoplanetary disks, which have narrow lines. These disks, however, are very small and are barely resolved even with the largest interferometers. Their lines are very weak and, so far, only a score of molecular species have been identified there. Those species, of course, include CO, HCN, HCO^+, H_2O, NH_3, H_2S, SO (Phuong et al., 2018), but also formaldehyde, methyl cyanide, cyanoacetylene, formic acid and methanol. Many more will be detected with more sensitive searches in the near future.

The bricks essential for the construction of amino acids and the nucleobases seem therefore widespread across the Universe:

didn't Huygens prophetically write in *The Cosmotheoros: What's true in one part will hold over the whole Universe*? Does this mean they were originally accreted by the Earth from outer space? Not necessarily: it just shows those bricks form easily about everywhere and may survive in harsh environmental conditions. Most likely, they were already present in the pre-Solar nebula. They may have been destroyed by the Sun's ignition and the Earth's formation, but were quickly re-formed on the rocky/dusty surfaces of the young Earth and of a number of Solar System bodies, in particular meteorites and comets. The "Cometary Zoo" (**Figure 14**) observed on Comet Churyumov-Gerasimenko by the Rosetta space mission, seems to corroborate this view.

AUTHOR CONTRIBUTIONS

All authors listed have made a substantial, direct, and intellectual contribution to the work and approved it for publication.

REFERENCES

Ade, P. A. R., Aghanim, N., Arnaud, M., Baccigalupi, C., Banday, A. J., Barreiro, R. B., et al. (2016). The Planck List of High-Redshift Source Candidates. *Astron. Astrophys.* 596, A100. doi:10.1051/0004-6361/201527206

Agúndez, M., Cernicharo, J., and Guélin, M. (2015a). Discovery of Interstellar Ketenyl (HCCO), a Surprisingly Abundant Radical. *Astron. Astrophys.* 577, L5. doi:10.1051/0004-6361/201526317

Agúndez, M., Cernicharo, J., de Vicente, P., Marcelino, N., Roueff, E., Fuente, A., et al. (2015b). Probing Non-polar Interstellar Molecules through Their Protonated Form: Detection of Protonated Cyanogen (NCCNH+). *Astron. Astrophys.* 579, L10. doi:10.1051/0004-6361/201526650

Agúndez, M., Marcelino, N., Tercero, B., Cabezas, C., de Vicente, P., and Cernicharo, J. (2021a). O-bearing Complex Organic Molecules at the Cyanopolyyne Peak of TMC-1: Detection of C2H3CHO, C2H3OH, HCOOCH3, and CH3OCH3. *Astron. Astrophys.* 649, L4. doi:10.1051/0004-6361/202140978

Agúndez, M., Cabezas, C., Tercero, B., Marcelino, N., Gallego, J. D., de Vicente, P., et al. (2021b). Discovery of the Propargyl Radical (CH2CCH) in TMC-1: One of the Most Abundant Radicals Ever Found and a Key Species for Cyclization to Benzene in Cold Dark Clouds. *Astron. Astrophys.* 647, L10. doi:10.1051/0004-6361/202140553

Allamandola, L. J., Tielens, A. G. G. M., and Barker, J. R. (1985). Polycyclic Aromatic Hydrocarbons and the Unidentified Infrared Emission Bands - Auto Exhaust along the Milky Way. *ApJ* 290, L25. doi:10.1086/184435

Alloin, D., Guilloteau, S., Barvainis, R., Antonucci, R., and Tacconi, L. (1997). The Gravitational Lensing Nature of the Cloverleaf Unveiled in CO (7-6) Line Emission. *Astron. Astrophys.* 321, 24.

Altwegg, K., Balsiger, H., and Fuselier, S. A. (2019). Cometary Chemistry and the Origin of Icy Solar System Bodies: The View after Rosetta. *Annu. Rev. Astron. Astrophys.* 57, 113–155. doi:10.1146/annurev-astro-091918-104409

Bañados, E., Mazzucchelli, C., Momjian, E., Eilers, A.-C., Wang, F., Schindler, J.-T., et al. (2021). The Discovery of a Highly Accreting, Radio-Loud Quasar at Z = 6.82. *ApJ* 909, 80. doi:10.3847/1538-4357/abe239

Barvainis, R., Maloney, P., Antonucci, R., and Alloin, D. (1997). Multiple CO Transitions, CI, and HCN from the Cloverleaf Quasar. *ApJ* 484, 69.

Belloche, A., Menten, K. M., Comito, C., Müller, H. S. P., Schilke, P., Ott, J., et al. (2008). Detection of Amino Acetonitrile in Sgr B2(N). *Astron. Astrophys.* 482, 179–196. doi:10.1051/0004-6361:20079203

ACKNOWLEDGMENTS

Bradford, C. M., Aguirre, J. E., Aikin, R., Bock, J. J., Earle, L., Glenn, J., et al. (2009). The Warm Molecular Gas Around the Cloverleaf Quasar. *ApJ* 705, 112–122. doi:10.1088/0004-637x/705/1/112

Burbidge, E. M., Burbidge, G. R., Fowler, W. A., and Hoyle, F. (1957). Synthesis of the Elements in Stars. *Rev. Mod. Phys.* 29, 547–650. doi:10.1103/revmodphys.29.547

Burkhardt, A. M., Long Kelvin Lee, K., Bryan Changala, P., Shingledecker, C. N., Cooke, I. R., Loomis, R. A., et al. (2021). Discovery of the Pure Polycyclic Aromatic Hydrocarbon Indene (C-C9h8) with GOTHAM Observations of TMC-1. *Astrophys. J. Lett.* 913, L18. doi:10.3847/2041-8213/abfd3a

Cernicharo, J., and Guélin, M. (1987). The Physical and Chemical State of HCL2. *Astron. Astrophys.* 176, 299.

Cernicharo, J., Guélin, M., and Askne, J. (1984). TMC 1-like Cloudlets in HCL 2. *Astron. Astrophys.* 138, 371.

Cernicharo, J., Heras, A. M., Tielens, A. G. G. M., Pardo, J. R., Herpin, F., Guélin, M., et al. (2001). [ITAL]Infrared Space Observatory's[/ITAL] Discovery of C[TINF]4[/TINF]H[TINF]2[/TINF], C[TINF]6[/TINF]H[TINF]2[/TINF], and Benzene in CRL 618. *ApJ* 546, L123–L126. doi:10.1086/318871

Cernicharo, J., Marcelino, N., Agúndez, M., Endo, Y., Cabezas, C., Bermúdez, C., et al. (2020a). Discovery of HC3O+ in Space: The Chemistry of O-Bearing Species in TMC-1. *Astron. Astrophys.* 642, L17. doi:10.1051/0004-6361/202039351

Cernicharo, J., Marcelino, N., Pardo, J. R., Agúndez, M., Tercero, B., de Vicente, P., et al. (2020b). Interstellar Nitrile Anions: Detection of C3N– and C5N– in TMC-1. *Astron. Astrophys.* 641, L9. doi:10.1051/0004-6361/202039231

Cernicharo, J., Marcelino, N., Agúndez, M., Bermúdez, C., Cabezas, C., Tercero, B., et al. (2020c). Discovery of HC4NC in TMC-1: A Study of the Isomers of HC3N, HC5N, and HC7N. *Astron. Astrophys.* 642, L8. doi:10.1051/0004-6361/202039274

Cernicharo, J., Cabezas, C., Endo, Y., Marcelino, N., Agúndez, M., Tercero, B., et al. (2021a). Space and Laboratory Discovery of HC3S+. *Astron. Astrophys.* 646, L3. doi:10.1051/0004-6361/202040013

Cernicharo, J., Cabezas, C., Bailleux, S., Margulès, L., Motiyenko, R., Zou, L., et al. (2021b). Discovery of the Acetyl Cation, CH3CO+, in Space and in the Laboratory. *Astron. Astrophys.* 646, L7. doi:10.1051/0004-6361/202040076

Cernicharo, J., Agúndez, M., Kaiser, R. I., Cabezas, C., Tercero, B., Marcelino, N., et al. (2021c). Discovery of Benzyne, O-C6h4, in TMC-1 with the QUIJOTE Line Survey. *Astron. Astrophys.* 652, L9. doi:10.1051/0004-6361/202141660

Cernicharo, J., Agúndez, M., Cabezas, C., Tercero, B., Marcelino, N., Pardo, J. R., et al. (2021d). Pure Hydrocarbon Cycles in TMC-1: Discovery of Ethynyl

Cyclopropenylidene, Cyclopentadiene, and Indene. *Astron. Astrophys.* 649, L15. doi:10.1051/0004-6361/202141156

Cernicharo, J., Agúndez, M., Cabezas, C., Marcelino, N., Tercero, B., Pardo, J. R., et al. (2021e). Discovery of CH2CHCCH and Detection of HCCN, HC4N, CH3CH2CN, and, Tentatively, CH3CH2CCH in TMC-1. *Astron. Astrophys.* 647, L2. doi:10.1051/0004-6361/202140434

Cernicharo, J., Cabezas, C., Agúndez, M., Tercero, B., Marcelino, N., Pardo, J. R., et al. (2021f). Discovery of Allenyl Acetylene, H2CCCHCCH, in TMC-1. *Astron. Astrophys.* 647, L3. doi:10.1051/0004-6361/202140482

Cernicharo, J., Agúndez, M., Kaiser, R. I., Cabezas, C., Tercero, B., Marcelino, N., et al. (2021g). Discovery of Two Isomers of Ethynyl Cyclopentadiene in TMC-1. *Astron. Astrophys.* 655, L1.

Cernicharo, J., Cabezas, C., Agúndez, M., Tercero, B., PardoMarcelino, J. R. N., Marcelino, N., et al. (2021h). TMC-1, the Starless Core Sulfur Factory: Discovery of NCS, HCCS, H2CCS, H2CCCS, and C4S and Detection of C5S. *Astron. Astrophys.* 648, L3. doi:10.1051/0004-6361/202140642

Cernicharo, J., Cabezas, C., Endo, Y., Agúndez, M., Tercero, B., Pardo, J. R., et al. (2021i). The sulphur Saga in TMC-1: Discovery of HCSCN and HCSCCH. *Astron. Astrophys.* 650, L14. doi:10.1051/0004-6361/202141297

Cernicharo, J., Agúndez, M., Kaiser, R. I., Cabezas, C., Tercero, B., Marcelino, N., et al. (2021j). Discovery of Two Isomers of Ethynyl Cyclopentadiene in TMC-1: Abundances of CCH and CN Derivatives of Hydrocarbon Cycles. *Astron. Astrophys.* 655, L1. doi:10.1051/0004-6361/202142226

Cernicharo, J., Agúndez, M., Cabezas, C., Tercero, B., Marcelino, N., Fuentetaja, R., et al. (2021k). Discovery of HCCCO and C5O in TMC-1 with the QUIJOTE Line Survey. *Astron. Astrophys.*. 656, L21. doi:10.1051/0004-6361/202142634

Cernicharo, J. (2004). The Polymerization of Acetylene, Hydrogen Cyanide, and Carbon Chains in the Neutral Layers of Carbon-Rich Proto-Planetary Nebulae. *ApJ* 608, L41–L44. doi:10.1086/422170

Cherchneff, I., Barker, J. R., and Tielens, A. G. G. M. (1992). Polycyclic Aromatic Hydrocarbon Formation in Carbon-Rich Stellar Envelopes. *ApJ* 401, 269. doi:10.1086/172059

Cheung, A. C., Rank, D. M., Townes, C. H., Thornton, D. D., and Welch, W. J. (1968). Detection of NH3 Molecules in the Interstellar Medium by Their Microwave Emission. *Phys. Rev. Lett.* 21, 1701–1705. doi:10.1103/physrevlett.21.1701

Cheung, A. C., Rank, D. M., Townes, C. H., Thornton, D. D., and Welch, W. J. (1969). Detection of Water in Interstellar Regions by its Microwave Radiation. *Nature* 221, 626.

Combes, F., Gupta, N., Muller, S., Balashev, S., Józsa, G. I. G., Srianand, R., et al. (2021). PKS1830-211: OH and Hi at Z = 0:89 and the First MeerKAT UHF Spectrum. *Astron. Astrophys.* 648, 116. doi:10.1051/0004-6361/202040167

Cordiner, M. A., Charnley, S. B., Kisiel, Z., McGuire, B. A., and Kuan, Y.-J. (2017). Deep K-Band Observations of TMC-1 with the Green Bank Telescope: Detection of HC7O, Nondetection of HC11N, and a Search for New Organic Molecules. *ApJ* 850, 187. doi:10.3847/1538-4357/aa970c

Douglas, A. E., and Herzberg, G. (1941). Note on CH+ in Interstellar Space and in the Laboratory. *ApJ* 94, 3. doi:10.1086/144342

Ferus, M., Laitl, V., Knizek, A., Kubelík, P., Sponer, J., and Kára, J. (2018). HNCO-based Synthesis of Formamide in Planetary Atmospheres. *Astron. Astrophys.* 616, 150. doi:10.1051/0004-6361/201833003

Fuente, A., Navarro, D. G., Caselli, P., Gerin, M., Kramer, C., Roueff, E., et al. (2019). Gas Phase Elemental Abundances in Molecular cloudS (GEMS). *Astron. Astrophys.* 624, A105. doi:10.1051/0004-6361/201834654

García, R. G., Gentaz, O., Baldino, M., and Torres, M. (2012). "An 8 GHz Digital Spectrometer for Millimeter-Wave Astronomy," in Proceedings of the SPIE: Millimeter, Submillimeter, and Far-Infrared Detectors and Instrumentation for Astronomy VI, Amstrdam, September 24, 2012, 8452.

Garcia, R. G., Gentaz, O., Baldino, M., and Torres, M. (2012). An 8 GHz Digital Spectrometer for Millimeter-Wave Astronomy. *SPIE* 8452E, 2TG.

García-Burillo, S., Graciá-Carpio, J., Guélin, M., Neri, R., Cox, P., Planesas, P., et al. (2006). A New Probe of Dense Gas at High Redshift: Detection of HCO + (5-4) Line Emission in APM 08279+5255. *ApJ* 645, L17–L20. doi:10.1086/506204

Green, S., Montgomery, J. A. J., and Thaddeus, P. (1974). Tentative Identification of U93.174 as the Molecular Ion N2H/+/. *ApJ* 193, L89. doi:10.1086/181639

Guélin, M., and Cernicharo, J. (1989). "Molecular Abundances in the Dense Interstellar and Circumstellar Clouds," in The Physics and Chemistry of Interstellar Molecular Clouds, Proceedings of the Symposium. Zermatt, Switzerland. Sept 22-25, 1988. Editors G. Winnewisser and J. T. Armstrong (Berlin: Springer-Verlag), Vol. 331, 337. Lecture Notes in Physics.

Guélin, M., Salomé, P., Neri, R., García-Burillo, S., Graciá-Carpio, J., Cernicharo, J., et al. (2007). Detection of HNC and Tentative Detection of CN at Z = 3.9. *Astron. Astrophys.* 462, L45–L48. doi:10.1051/0004-6361/20066555

Guélin, M., and Thaddeus, P. (1977). Tentative Detection of the C3N Radical. *ApJ* 212, L81. doi:10.1086/182380

Guélin, M., Green, S., and Thaddeus, P. (1978). Detection of the C4H Radical toward IRC +10216. *ApJ* 224, L27. doi:10.1086/182751

Guélin, M., Omont, A., Kramer, C., Cernicharo, J., Tercero, B., Yang, C., et al. (2022). in preparation. *Astron. Astrophys.*

Guilloteau, S., Delannoy, J., Downes, D., Greve, A., Guélin, M., Lucas, R., et al. (1992). The IRAM interferometer on Plateau de Bure. *Astron. Astrophys.* 262, 6.

Herbst, E., and Klemperer, W. (1974). Is X-Ogen HCO+? *ApJ* 188, 255. doi:10.1086/152712

Hodge, J. A., and da Cunha, E. (2020). *High-redshift star Formation in the ALMA Era.* arXiv:2004.00934, 7 (12). Royal Society Open Science.

Holtom, P. D., Bennett, C. J., Osamura, Y., Mason, N. J., and Kaiser, R. I. (2005). A Combined Experimental and Theoretical Study on the Formation of the Amino Acid Glycine (NH2CH2COOH) and its Isomer (CH3NHCOOH) in Extraterrestrial Ices. *ApJ* 626, 940–952. doi:10.1086/430106

Hoyle, F. (1957). *The Black Cloud.* London: William Heinemann Ltd.

Huygens, C. (1698). *Cosmotheoros, Book I Adriaan Moetjens.* The Hague.

Jiménez-Serra, I., Martín-Pintado, J., Rivilla, V. M., Rodríguez-Almeida, L., Alonso Alonso, E. R., Zeng, S., et al. (2020). Toward the RNA-World in the Interstellar Medium-Detection of Urea and Search of 2-Amino-Oxazole and Simple Sugars. *Astrobiology* 20, 1048–1066. doi:10.1089/ast.2019.2125

Joblin, C., and Cernicharo, J. (2018). Detecting the Building Blocks of Aromatics. *Science* 359, 156–157. doi:10.1126/science.aar4541

Kaifu, N., Ohishi, M., Kawaguchi, K., Saito, S., Yamamoto, S., Miyaji, T., et al. (2004). A 8.8-50 GHz Complete Spectral Line Survey toward TMC-1 I. Survey Data. *Publ. Astron. Soc. Jpn.* 56, 69–173. doi:10.1093/pasj/56.1.69

Kneib, J. P., Alloin, D., and Pello, R. (1998). Unveiling the Nature of the Cloverleaf Lens-System: HST/NICMOS-2 Observations. *Astron. Astrophys.* 339, L65.

Léger, A., and Puget, J. L. (1984). Identification of the "unidentified" IR Emission Features of Interstellar Dust? *Astron. Astrophys.* 137, L5.

Kelvin Lee, K. L., Changala, P. B., Loomis, R. A., Burkhardt, A. M., Xue, C., Cordiner, M. A., et al. (2021). Interstellar Detection of 2-cyanocyclopentadiene, C5H5CN, a Second Five-Membered Ring toward TMC-1. *Astrophys. J. Lett.* 910, L2. doi:10.3847/2041-8213/abe764

Lidman, C., Courbin, F., Meylan, G., Broadhurst, T., Frye, B., and Welch, W. J. W. (1999). The Redshift of the Gravitationally Lensed Radio Source PKS 1830–211. *ApJ* 514, L57–L60. doi:10.1086/311949

Marcelino, N., Cernicharo, J., Agúndez, M., Roueff, E., Gerin, M., Martín-Pintado, J., et al. (2007). Discovery of Interstellar Propylene (CH 2 CHCH 3): Missing Links in Interstellar Gas-phase Chemistry. *ApJ* 665, L127–L130. doi:10.1086/521398

Marcelino, N., Agúndez, M., Tercero, B., Cabezas, C., Bermúdez, C., Gallego, J. D., et al. (2020). Tentative Detection of HC5NH+ in TMC-1. *Astron. Astrophys.* 643, L6. doi:10.1051/0004-6361/202039251

Martínez, L., Santoro, G., Merino, P., Accolla, M., Lauwaet, K., Sobrado, J., et al. (2020). Prevalence of Non-aromatic Carbonaceous Molecules in the Inner Regions of Circumstellar Envelopes. *Nat. Astron.* 4, 97–105. doi:10.1038/s41550-019-0899-4

Martin, S., Mauersberger, R., Martin-Pintado, J., Henkel, C., and Garcia-Burillo, S. (2006). A 2 Millimeter Spectral Line Survey of the Starburst Galaxy NGC 253. *Astrophys J. Suppl. S* 164, 450–476. doi:10.1086/503297

Matthews, H. E., Irvine, W. M., Friberg, P., Brown, R. D., and Godfrey, P. D. (1984). A New Interstellar Molecule: Triearbon Monoxide. *Nature* 310, 125–126. doi:10.1038/310125a0

McCarthy, M. C., Lee, K. L. K., Loomis, R. A., Burkhardt, A. M., Shingledecker, C. N., Charnley, S. B., et al. (2021). Interstellar Detection of the Highly Polar Five-Membered Ring Cyanocyclopentadiene. *Nat. Astron.* 5, 176–180. doi:10.1038/s41550-020-01213-y

McGuire, B. A., Burkhardt, A. M., Shingledecker, C. N., Kalenskii, S. V., Herbst, E., Remijan, A. J., et al. (2017). Detection of Interstellar HC 5 O in TMC-1 with the Green Bank Telescope. *ApJ* 843, L28. doi:10.3847/2041-8213/aa7ca3

McGuire, B. A., Burkhardt, A. M., Kalenskii, S., Shingledecker, C. N., Remijan, A. J., Herbst, E., et al. (2018). Detection of the Aromatic Molecule Benzonitrile (C -C 6 H 5 CN) in the Interstellar Medium. *Science* 359, 202–205. doi:10.1126/science.aao4890

McGuire, B. A., Loomis, R. A., Burkhardt, A. M., Lee, K. L. K., Shingledecker, C. N., Charnley, S. B., et al. (2021). Detection of Two Interstellar Polycyclic Aromatic Hydrocarbons via Spectral Matched Filtering. *Science* 371, 1265–1269. doi:10.1126/science.abb7535

McGuire, B. A. (2018). Census of Interstellar, Circumstellar, Extragalactic, Protoplanetary Disk, and Exoplanetary Molecules. *ApJS* 239, 1. doi:10.3847/1538-4365/aae5d2

McKellar, A. (1940). Evidence for the Molecular Origin of Some Hitherto Unidentified Interstellar Lines. *PASP* 52, 187. doi:10.1086/125159

Muller, S., and Guélin, M. (2008). Drastic Changes in the Molecular Absorption at Redshift Z = 0.89 toward the Quasar PKS 1830-211. *Astron. Astrophys.* 491, 739–746. doi:10.1051/0004-6361:200810392

Muller, S., Guélin, M., Dumke, M., Lucas, R., and Combes, F. (2006). Probing Isotopic Ratios Atz= 0.89: Molecular Line Absorption in Front of the Quasar PKS 1830-211. *Astron. Astrophys.* 458, 417–426. doi:10.1051/0004-6361:20065187

Muller, S., Beelen, A., Guélin, M., Aalto, S., Black, J. H., Combes, F., et al. (2011). Molecules at Z = 0.89: A 4-Mm-Rest-Frame Absorption-Line Survey toward PKS 1830-211. *Astron. Astrophys.* 535, 32. doi:10.1051/0004-6361/201117096

Muller, S., Combes, F., Guélin, M., Gérin, M., Aalto, S., Beelen, A., et al. (2014). An ALMA Early Science Survey of Molecular Absorption Lines toward PKS 1830-211. Analysis of the Absorption Profiles. *Astron. Astrophys.* 566, 21. doi:10.1051/0004-6361/201423646

Muller, S., Müller, H. S. P., Black, J. H., Beelen, A., Combes, F., Curran, S., et al. (2016). OH$^+$ and H$_2$O$^+$ Absorption towards PKS 1830-211. *Astron. Astrophys.* 595, A128. doi:10.1051/0004-6361/201629073

Muller, S., Müller, H. S. P., Black, J. H., Gérin, M., Combes, F., and Curran, S. (2017). Detection of CH+, SH+, and Their 13C- and 34S-Isotopologues toward PKS 1830-211. *Astron. Astrophys.* 606, 109. doi:10.1051/0004-6361/201731405

Muller, S., Roueff, E., Black, J. H., Gérin, M., Guélin, M., Menten, K., et al. (2020). Detection of Deuterated Molecules, but Not of Lithium Hydride, in the Z = 0.89 Absorber toward PKS 1830-211. *Astron. Astrophys.* 637, A7. doi:10.1051/0004-6361/202037628

Ohishi, M., Ishikawa, S.-I., Yamada, C., Kanamori, H., Irvine, W. M., Brown, R. D., et al. (1991). Detection of a New Carbon-Chain Molecule, CCO. *ApJ* 380, L39. doi:10.1086/186168

Pensabene, A., Decarli, R., Bañados, E., Venemans, B., Walter, F., and Bertoldi, F. (2021). An ALMA Multi-Line Survey of the ISM in Two Quasar Host–Companion Galaxy Pairs at z > 6. *Astron. Astrophys.* 652, A66.

Phuong, N. T., Chapillon, E., Majumdar, L., Dutrey, A., Guilloteau, S., Piétu, V., et al. (2018). First Detection of H2S in a Protoplanetary Disk. *Astron. Astrophys.* 616, L5. doi:10.1051/0004-6361/201833766

Pilleri, P., Joblin, C., Boulanger, F., and Onaka, T. (2015). Mixed Aliphatic and Aromatic Composition of Evaporating Very Small Grains in NGC 7023 Revealed by the 3.4/3.3μm Ratio. *Astron. Astrophys.* 577, A16. doi:10.1051/0004-6361/201425590

Reuter, C., Vieira, J. D., Spilker, J. S., Weiss, A., Aravena, M., Archipley, M., et al. (2020). The Complete Redshift Distribution of Dusty Star-forming Galaxies from the SPT-SZ Survey. *ApJ* 902, 78. doi:10.3847/1538-4357/abb599

Rivilla, V. M., Martín-Pintado, J., Jiménez-Serra, I., Zeng, S., Martín, S., Armijos-Abendaño, J., et al. (2019). Abundant Z-Cyanomethanimine in the Interstellar Medium: Paving the Way to the Synthesis of Adenine. *MNRAS* 483, 114. doi:10.1093/mnrasl/sly228

Robintaille, T. P., and Whitney, B. A. (2010). The Present-Day star Formation Rate of the Milky-Way Determined from Spitzer Detected Young Stellar Objects. *ApJ* 710, L11. doi:10.1088/2041-8205/710/1/L11

Rubin, R. H., Swenson, G. W. J., Jr., Benson, R. C., Tigelaar, H. L., and Flygare, W. H. (1971). Microwave Detection of Interstellar Formamide. *ApJ* 169, L39. doi:10.1086/180810

Shingledecker, C. N., Lee, K. L. K., Wandishin, J. T., Balucani, N., Burkhardt, A. M., Charnley, S. B., et al. (2021). Detection of Interstellar H2CCCHC3N. *Astron. Astrophys.* 652, L12. doi:10.1051/0004-6361/202140698

Snyder, L. E., Buhl, D., Zuckerman, B., and Palmer, D. (1969). Microwave Detection of Interstellar Formaldehyde. *Phys. Rev. L.* 22, 679.

Snyder, L. E., Lovas, F. J., Hollis, J. M., Friedel, D. N., Jewell, P. R., Remijan, A., et al. (2005). A Rigorous Attempt to Verify Interstellar Glycine. *ApJS* 108, 301. doi:10.1086/426677

Solomon, P., Vanden Bout, P., Carilli, C., and Guélin, M. (2003). The Essential Signature of a Massive Starburst in a Distant Quasar. *Nature* 426, 636. doi:10.1038/nature02149

Spilker, J. S., Marrone, D. P., Aguirre, J. E., Aravena, M., Ashby, M. L. N., Béthermin, M., et al. (2014). The Rest-Frame Submillimeter Spectrum of High-Redshift, Dusty, Star-forming Galaxies. *ApJ* 785, 149. doi:10.1088/0004-637x/785/2/149

Spilker, J. S., Marrone, D. P., Aravena, M., Béthermin, M., Bothwell, M. S., Carlstrom, J. E., et al. (2016). ALMA Imaging and Gravitational Lens Models of South Pole Telescope –Selected Dusty, Sta-Forming Galaxies at High Redshifts. *ApJ* 826, 112. doi:10.3847/0004-637x/826/2/112

Stacey, H. R., McKean, J. P., Powell, D. M., Vegetti, S., Rizzo, F., and Spingola, C. (2021). The Rocky Road to Quiescence: Compaction and Quenching of Quasar Host Galaxies. *MNRAS* 500, 3667. doi:10.1093/mnras/staa3433

Swings, P., and Rosenfeld, L. (1937). Considerations Regarding Interstellar Molecules. *ApJ* 86, 4. doi:10.1086/143880

Tercero, B., Cernicharo, J., Pardo, J. R., and Goicoechea, J. (2010). A Line Confusion Limited Millimeter Survey of Orion KL. I. Sulfur Carbon Chains. *Astron. Astrophys.* 517, A96. doi:10.1051/0004-6361/200913501

Tercero, B., Cernicharo, J., Cuadrado, S., de Vicente, P., and Guélin, M. (2020). New Molecular Species at Redshift Z = 0.89. *Astron. Astrophys.* 636, L7. doi:10.1051/0004-6361/202037837

Tercero, F., López-Pérez, J. A., Gallego, J. D., Beltrán, F., García, O., Patino-Esteban, M., et al. (2021). Yebes 40 M Radio Telescope and the Broad Band Nanocosmos Receivers at 7 Mm and 3 Mm for Line Surveys. *Astron. Astrophys.* 645, 37. doi:10.1051/0004-6361/202038701

Thaddeus, P. (2006). The Prebiotic Molecules Observed in the Interstellar Gas. *Phil. Trans. R. Soc. B* 361, 1681. doi:10.1098/rstb.2006.1897

Tucker, K. D., Kutner, M. L., and Thaddeus, P. (1974). The Ethynyl Radical C2H-A New Interstellar Molecule. *ApJ* 193, L115. doi:10.1086/181646

Venturini, S., and Solomon, P. L. (2003). The Molecular Disk in the Cloverleaf Quasar. *ApJ* 590, 740. doi:10.1086/375050

Voltaire (1752). *Micromegas Les Editions de Londres.*

Wang, F., Yang, J., Fan, X., Hennawi, J. F., Barth, A. J., Banados, E., et al. (2021). A Luminous Quasar at Redshift 7.642. *ApJ* 907, L1. doi:10.3847/2041-8213/abd8c6

Weiss, A., De Breuck, C., Marrone, D. P., Vieira, J. D., Aguirre, J. E., Aird, K. A., et al. (2013). ALMA Redshifts of Millimeter-Selected Galaxies from the SPT Survey: The Redshift Distribution of Dusty Star-forming Galaxies. *ApJ* 767, 88. doi:10.1088/0004-637X/767/1/88

Wildy, C., and Czerny, B. (2017). The Relationship between Mg II Broad Emission and Quasar Inclination Angle. *FASS* 4, 43. doi:10.3389/fspas.2017.00043

Wilson, R. W., Jefferts, K. B., and Penzias, A. A. (1970). Carbon Monoxide in the Orion Nebula. *ApJ* 161, L43. doi:10.1086/180567

Winn, J., Kochanek, C., McLeod, B., Falco, E., Impey, C. D., and Rix, H. W. (2002). PKS 1830-211: A Face-On Spiral Galaxy Lens. *ApJ* 575, 103. doi:10.1086/341265

Woods, P. M., Millar, T. J., Zijlstra, A. A., and Herbst, E. (2002). The Synthesis of Benzene in the Proto-Planetary Nebula CRL 618. *ApJ* 574, L167. doi:10.1086/342503

Yang, C., Omont, A., Beelen, A., González-Alfonso, E., Neri, R., Gao, Y., et al. (2016). H$_2$O and H$_2$O$^+$ Emission in Lensed Hy/ULIRGs at Z=2-4. *Astron. Astrophys.* 595, A8. doi:10.1051/0004-6361/201628160

Yang, C., Gavazzi, A., and Beelen, A. (2019). CO, H$_2$O, H$_2$O$^+$ Line and Dust Emission in a z=3.63 Strongly Lensed Starburst Merger at Sun-Kiloparsec Scales. *Astron. Astrophys.* 624, 138. doi:10.1051/0004-6361/201833876

Yang, C., González-Alfonso, E., Omont, A., Pereira-Santaella, M., Fischer, J., Beelen, A., et al. (2020). First Detection of the 448 GHz Ortho-H$_2$O Line at High Redshift. *Astron. Astrophys.* 634, L3. doi:10.1051/0004-6361/201937319

Zeng, S., Quénard, D., Jiménez-Serra, I., Martín-Pintado, J., Rivilla, V. M., Testi, L., et al. (2019). First Detection of the Pre-biotic Molecule Glycolonitrile (HOCH$_2$CN) in the Interstellar Medium. *MNRAS* 484, L43. doi:10.1093/mnrasl/slz002

Zhang, Z. Y., Romano, D., Ivinson, R. J., Papadopoulos, P. P., and Matteucci, F. (2018). Stellar Populations Dominated by Massive Stars in Dusty Starburst Galaxies across Cosmic Time. *Nature* 558, 260. doi:10.1038/s41586-018-0196-x

Conflict of Interest: The authors declare that the research was conducted in the absence of any commercial or financial relationships that could be construed as a potential conflict of interest.